Article

Journal of
Nanoscience and Nanotechnology
Vol. 20, 5964–5969, 2020
www.aspbs.com/jnn

Investigation of Photocatalytic Efficiency of Supported CuO Nanoparticles on Natural Zeolite Particles in Photodegradation of Methyl Orange

Hassan Koohestani*, Hamed Mansouri, Abbas Pirmoradian, and Mohammad Hassanabadi

Faculty of Materials and Metallurgical Engineering, Semnan University, Semnan, 35131-19111, Iran

In the current work, CuO nanoparticles were deposited on natural zeolite's particles to resolve the drawbacks of zeolite catalysis. The synthesized composites were characterized by XRD, SEM, BET, and DRS analyses. The results illustrated that in the 15% CuO composite, CuO nanoparticles with a size of 21 nm are deposited on the surface of the zeolite particles. Deposition of CuO nanoparticles on zeolite's particles decreased the specific surface area from 35 m^2/g (pure zeolite) to 28 m^2/g (20% CuO composite), and causes a red shift in the absorption edge of the sample to 796 nm for 20% CuO composite. In order to compare the samples' performances in eliminating water pollutants, methyl orange dye removal was investigated. The analyses indicated that the optimum efficiency (85% in 120 min) belongs to zeolite-15% CuO composite with a band gap of 1.70 eV.

Keywords: Natural Zeolite, CuO, Photocatalytic Activity, Dye Removal.

1. INTRODUCTION

In many industries wastewaters containing organic compounds and non-organic materials are formed and are later discharged into water and soil [1–3]. The azo dye as synthetic colorants in various industries is one of the most common and harmful industrial pollutants [4]. Therefore, these pollutants are extremely dangerous effect for body life especially human life. Increased demand to safe water caused to treating water and destructing these pollutants and returning them to the consumption cycle [3, 5]. To this end, different methods, such as biodegradation, filtration, precipitation, solvent extraction, ion exchange and electrochemical treatment have been applied [3]. However, these conventional methods have some drawbacks such as: high-energy requirements, incomplete ion removal and production of toxic sludge. One of the new methods of removing the pollutants from water is using mineral absorbents such as zeolite [3, 6, 7].

Zeolite is a mineral material consisting of alumina and silica, has unique properties such as high cation exchange capacity, high adsorption capacity etc. [8]. As a result its high absorption, zeolite is used in refineries to remove or destruct harmful materials. Zeolite has been studied and used in two forms of natural and artificial [5, 9–11]. Natural zeolite is cost effective and more eco-friendly [8]. Despite its unparalleled properties, zeolite application is accompanied with some problems. One of the problems of using zeolite is its reduced absorption ability due to being saturated by the pollutants. Therefore, zeolite is required to be recycled [12–14]. On the other hand, the efficiency of absorbing and destructing the pollutants by zeolite needs to be enhanced to reach an optimum. Consequently, researchers have coated zeolite by various photocatalysts including Pt-TiO_2, TiO_2, Ni/Pb sulfide, Zn(II)/Cu(II) oxides, NiS-P, ZnO, and Fe^{3+}-TiO_2 in order to increase natural zeolite's absorption ability [1, 8, 14–19].

Photocatalysts are semiconductor compounds. When a photocatalyst absorb a light with at least as much energy as its band gap energy, electron–hole pairs are produced in it. The resulted holes can oxidize water on the semiconductor's surface and powerful hydroxyl radicals ($OH^{\cdot}$) are produced. On the other hand, produced electrons react with absorbed oxygen to create superoxide radical anions ($O_2^{\cdot-}$). These radicals can attack to the pollutants existing in the water to degrade [13, 20, 21]. Thus, depositing photocatalyst on the surface of the zeolite's particles

*Author to whom correspondence should be addressed.

 1533-4880/2020/20/5964/006 doi:10.1166/jnn.2020.18548

will lead to benefiting from them both in removing the pollutants [16, 17, 22].

CuO is one of the photocatalysts available. CuO is a semiconductor of type P with a narrow band energy (1.2 eV), and a high capability to absorb UV light [23, 24]. CuO/Zeolite sandwich type absorbent-catalyst was prepared through wet impregnation of synthesized zeolite. Then sandwich used to oxidize alcohols in form of CO_2 and H_2O [22, 25]. Various researchers have studied the influence of CuO on the performance of different types of synthesized zeolites and they have all reported the positive effect of CuO on zeolite's efficiency [25, 26]. Although CuO improves the absorption ability of natural zeolites under the radiation of UV-vis light, very limited research has been done on depositing CuO nanoparticles on natural zeolite. Therefore, the aims of the current work are to produce a CuO catalyst supported on natural zeolite by precipitation process and to investigate its adsorption and photocatalytic performance for the removal of methyl orange (MO) under UV-vis light.

2. EXPERIMENTAL DETAILS

2.1. Materials

Natural zeolite of clinoptilolite + cristobalite + quartz with the composition presented in Table I was obtained from Afrazand-e Semnan Company. Copper (II) sulfate ($CuSO_4 \cdot 5H_2O$), sodium hydroxide (NaOH), ascorbic acid ($C_6H_8O_6$), and methyl orange were purchased from Merck company.

2.2. Coating of Zeolite's Particles by Nanoparticles of CuO

To produce the composite of zeolite/CuO, CuO nanoparticles were synthesised by using a chemical method as described in our previous work [23, 27]. In brief, 0.4 g of $CuSO_4 \cdot 5H_2O$ was added to 100 ml of deionized water and stirred for 20 min by a magnetic stirrer. Next, 30 ml of sodium hydroxide 0.05 M was dripped into the solution. After 30 min of stirring a dark blue solution was obtained. Then 30 ml of ascorbic acid 0.05 M was then dripped to the solution. Afterwards, a certain amount of natural zeolite which was earlier washed by ethanol and deionized water and then dried was added to the solution. The amount of zeolite added was adjusted to obtain four samples with %CuO = 5%, 10%, 15% and 20% (were named as Z-5C, Z-10C, Z-15C and Z-20C). The solution was stirred for 1 h. After some time (approximately 2 h), the deposited powder was collected, which was first dried for 1 h at 60 °C, and then calcined for 2 h at 250 °C.

Table I. Chemical analysis of used natural zeolite.

Components	SiO_2	Al_2O_3	Fe_2O_3	CaO	Na_2O	K_2O
% wt	67.82	10.91	0.65	0.89	3.85	4.07

2.3. Characterization of Zeolite/CuO Composite

The crystalline phases of the synthesized samples were studied by X-ray diffractometer (XRD, Bruker D8, Germany) with monochromated Cu–Kα radiation (λ = 1.54056 Å). The morphology of the particles was examined by a scanning electron microscope (SEM, XL 30-Philips, Netherlands). In order to determine the chemical composition, and molecular structure, and to identify the organic compounds, and the agent groups of the particles on the surface, infrared spectroscopy (FTIR) was conducted in the frequency range of 400–4000 cm^{-1} by ABB-Bomem model MB-100 instrument. The specific surface area of the synthesized samples was determined by BET surface analyzer (Belsorp mini II; Bel, Japan). Light absorbance spectra of the composite were measured by using a UV-Vis spectrophotometer (Avantes, Avaspec-2048-TEC) at room temperature. Band gap energy (E_g, eV) of samples was calculated by using the following equation [28]:

$$E_g = \frac{1243}{\lambda_g} \quad (1)$$

Where, the absorption onset wavelength (λ_g, nm) is the crossing point between the line extrapolated from the onset of the rising part of the absorbance spectra and x-axis of the plot [29, 30].

2.4. Photocatalytic Performance of the Zeolite/CuO Composite

Methyl orange (MeO) was used to investigate the photocatalytic performance of the Zeolite/CuO composite. MeO solution (50 ml) with the initial concentration of 5 ppm was prepared in a cylindrical glass vessel. The Zeolite/CuO composite (150 ppm) was added to the dye solution. Throughout the examination the temperature of the glass vessel was maintained constant at 25 °C. Before the radiation started, MeO solution was stirred for 1 h in a dark room to achieve the absorption-desorption equilibrium.

Subsequently, the system was placed under the radiation UV light provided by two 6 W UVC lamp (T5 fluorescent light, China) which vertical irradiate on the dye solution. The distance between the surface of the solution and the lamps was 10 cm. Samples were taken out from the solution at 30 min intervals during the radiation. Changes in the concentration of MeO were determined by spectrophotometer UV-vis instrument (6705; Jenway, UK) at the maximum absorption wavelength 462 nm.

The extent of dye removal efficiency was calculated by the following equation [31]:

$$\eta\% = \left(\frac{C_0 - C}{C_0}\right) \times 100 \quad (2)$$

Where C_0 is the initial dye concentration in the solution, and C is the dye concentration at the time of t.

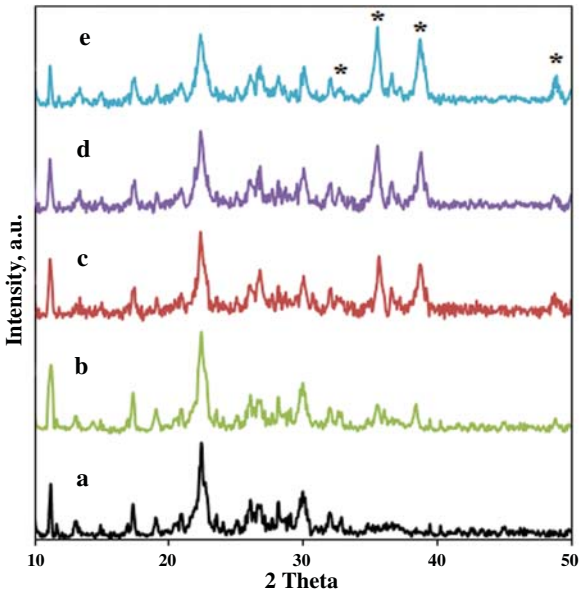

Figure 1. XRD pattern of samples ((a) natural zeolite, (b) Z-5C, (c) Z-10C, (d) Z-15C, (e) Z-20C and *CuO peak).

3. RESULTS AND DISCUSSION

Figure 1 shows the X-ray diffraction pattern for the natural zeolite and zeolite-CuO composites. The peaks in zeolite pattern in Figure 1(a) indicate the presence of three phases of clinopetiolite, cristobalite, and quartz [1]. In Figures 1(b) to (e), which is related to Z-5C to Z-20C composites, in addition to the existing phases in zeolite, the peaks related to CuO have also been identified (JCPDS Card No. 01-080-1916 for CuO). Some of these peaks were observed at the angles of $2\theta = 32.6, 35.8, 38.9$ and 48.8. As the amount of CuO increases, the peak intensities increase. It is obvious that the diffraction peak of CuO plates are considerably broadened, which demonstrate a smaller crystallite size [32]. CuO crystallite size in Z-15C sample was determined to be 21 nm through Scherrer equation.

Morphology images of natural zeolite and Z15C composite are illustrated in Figure 2. As it can be seen, zeolite particles are big in size. In Figure 2(b), CuO particles with the sizes of 30 to 80 nm have coated zeolite's surface. The images suggest that the particles have stuck together and have been agglomerated, which reduces the specific surface area. Nezamzadeh and Salimi [25] reported the same result in his analysis concerning the effect of CuO on synthesized zeolite. However, it has been shown that adding CuO to synthesized zeolite leads to a decrease in the size of zeolite's pores and increases active locations in the catalyst [33].

Infrared spectroscopy diagram depicts the type of surface and molecular bonds. Figure 3 displays FTIR spectrum related to Z15C sample. Peaks in the range of 400–800 cm^{-1} relate to the tensile vibrations of metal-oxygen bonds (Cu–O, Si–O and Al–O) [22, 34]. The generated vibrations of Al–O bonds and Si–O–Si asymmetric stretching are situated at 1041 cm^{-1} [35]. The peak in the range of 1632 cm^{-1} corresponds with the tensile vibration of H–O–H bond. The other peak at 3665 cm^{-1} which is relatively wide is due to bridging OH groups in Al–OH–Si and is attributed to the location of hydrogen atoms on different oxygen atoms of zeolite framework [35]. The intensities associated with the Si–O and O–Al bonds are very strong, which suggests that the zeolite has a large surface area [34, 36]. FTIR spectra show also some peaks at 3015, 2920 and 1438 cm^{-1} which, respectively, relate to C–H, C–C and N–C vibrations of the organic components [37].

BET result in Table II demonstrates that in Zeolite/CuO composites, the distribution of CuO on zeolite has caused a change in the specific surface area. A large portion of the specific surface area in the composites belongs to zeolite, and depositing CuO fills the porosities and hence reduces the specific surface area. According to the results, as the amount of CuO rises, there will be a greater decline in the specific surface area in a way that in 20% of CuO, the specific surface area drops to 28 m^2/g whereas the specific surface area of the pure zeolite is 35 m^2/g.

It is widely known that optical properties of the materials strongly influence their photocatalytic performance. Therefore, band gap as one of the most important optical properties of the photocatalysts will be analyzed first. Spectrometry UV-vis diffuse reflectance curves of the synthesized composites has been shown in Figure 4.

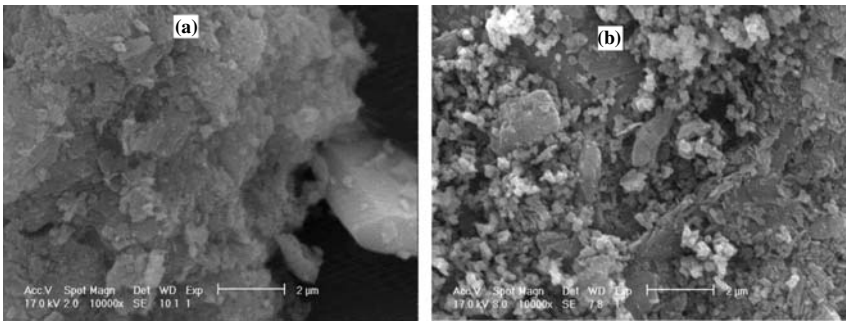

Figure 2. SEM image of (a) used natural Zeolite and (b) Zeolite/15% CuO.

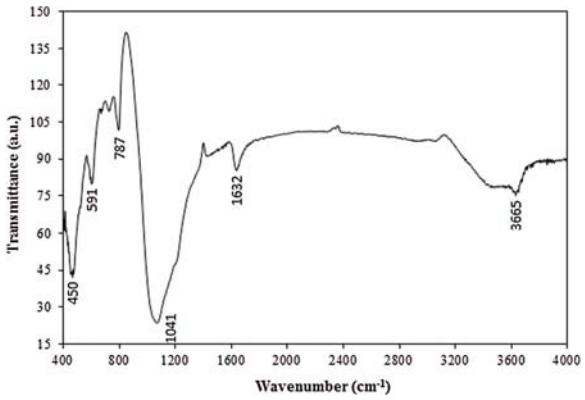

Figure 3. FT-IR spectra of Zeolite/15% CuO.

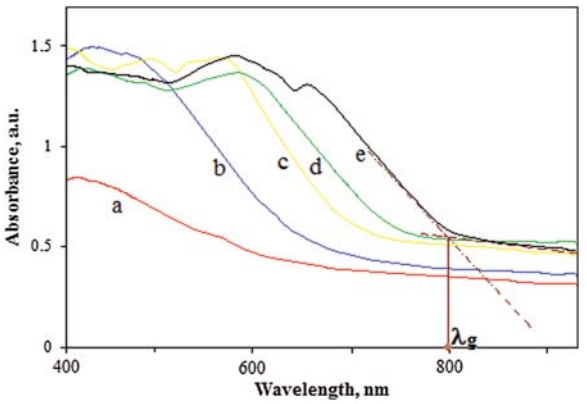

Figure 4. Diffuse UV-vis absorbance spectra of samples ((a) zeolite, (b) Z-5C, (c) Z-10C, (d) Z-15C, (e) Z-20C).

The absorption onset wavelength (λ_g) and corresponding band gap energy (E_g) of the samples were obtained by Eq. (1) and the onset from the cross of the straight line of the absorption onset with the baseline of the spectrum at longer wavelengths (similar Fig. 4) are summarized in Table II. Pure zeolite has not demonstrated any absorption in the wavelengths above 240 nm, while adding nanoparticles of CuO has resulted in absorption in high wavelengths in such a way that adding more CuO will shift the absorption edge to higher wavelengths, and in the sample of Z-20C the absorption edge has reached the amount of 796 nm and band gap is its lowest amount (1.56 eV). However, the absorption edge and band gap in pure CuO have been reported to be 882 nm and 1.37 eV, respectively. In other investigations it has been clarified that pure zeolite in the UV-vis area does not indicate any absorption, and adding different semiconducting photocatalysts causes a transition and red shifting in its absorption edge.

Methyl orange dye was removed by Zeolite/CuO composites under the radiation of UV-vis light in order to compare and evaluate the photocatalytic performance of these composites. Figure 5 represents the efficiency of removing MeO dye by different Zeolite/CuO composites under the radiation of UV light. It is evident that zeolite has a low efficiency which is in fact due to absorption properties of zeolite since it has been shown that zeolite does not possess photocatalytic properties. Zeolite/CuO composites are of higher efficiency compared to zeolite because they benefit from the absorption properties of zeolite as well as photocatalytic properties of CuO. However, the capability of the samples to remove MeO is different which is owing to the differences in surface charge of the particles, the specific surface area, and band energy. The highest efficiency belongs to Z-15C (85%). In higher amounts of CuO as a larger area of zeolite particles is coated by CuO nanoparticles, the absorption removal of the dye by zeolite reduces relatively. Consequently, photocatalytic removal is the better choice. Moreover, since CuO alone does not have a good photocatalytic performance because of its low rate of charge-transfer, it was expected that in high amounts of CuO the performance of Zeolite/CuO composite would deteriorate. This has been confirmed by other researchers [9, 15, 26]. Degradation of methyl orange has been studied by using the GC-mass in some research. Formation of N,N'-dimethyl-p-phenylenediamine ($m/z = 136$), 4-amino sulfonic acid ($m/z = 177$) and etc. were reported as the degradation products of MO. The research also confirmed that degradation intermediates of methyl orange are less toxic than the primary MO dye [38, 39].

Table II. Physical properties of the synthesized zeolite/CuO composites.

	Specific surface area, m^2/g	Absorption edge wavelength, nm	Band gap, eV
Z	35	–	–
Z-5C	33	625	1.98
Z-10C	32	680	1.82
Z-15C	29	732	1.70
Z-20C	28	796	1.56

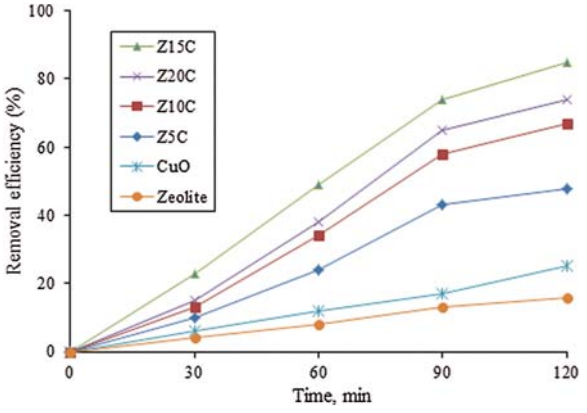

Figure 5. Removal efficiency of MeO by different samples.

The adsorption capacity of the samples, q_t (mg/g), can be obtained using the equation [37]:

$$q_t = \frac{(C_o - C_e)V}{m} \quad (3)$$

q_t is the quantity of dye adsorbed per unit mass of adsorbent at time t (mg/g), V is the volume of the dye solution and m is the mass of adsorbent. C_o and C_e are the initial and equilibrium dye concentrations (mg/L), respectively. The maximum adsorption capacities of the zeolite and Z-15C for MO degradation are determined to be 29.7 and 6.2 mg/g, respectively, which shows that the CuO nanoparticles supported on natural zeolite performs considerably better than the zeolite.

4. CONCLUSION

In the current work, in order to improve zeolite's performance in removing the pollutants from water, CuO nanoparticles were successfully deposited on natural zeolite's particles. The composite was examined by XRD, SEM, BET, and DRS analyses. The performances of the produced composites were compared according to their ability to remove methyl orange. The results demonstrated that depositing CuO nanoparticles promotes zeolite's efficiency in removing the pollutants, since CuO has photocatalytic properties and is capable of absorbing UV-vis light. The optimum efficiency was observed in the Z-15C composite.

Acknowledgments: The authors would like to thank the Afrazand-e Semnan Company for the supply of natural zeolite. We also appreciate Mr Rajabi for advice and guidance.

References and Notes

1. Koohestani, H., Hassanabadi, M., Mansouri, H. and Pirmoradian, A., **2019**. Investigation of photocatalytic performance of natural zeolite/TiO_2 composites. *Micro and Nano Letters*, *14*, pp.669–673.
2. Kabra, K., Chaudhary, R. and Sawhney, R.L., **2004**. Treatment of hazardous organic and inorganic compounds through aqueous-phase photocatalysis: A review. *Industrial & Engineering Chemistry Research*, *43*(24), pp.7683–7696.
3. Derikvandi, H. and Nezamzadeh-Ejhieh, A., **2017**. Synergistic effect of pn heterojunction, supporting and zeolite nanoparticles in enhanced photocatalytic activity of NiO and SnO_2. *Journal of Colloid and Interface Science*, *490*, pp.314–327.
4. Senobari, S. and Nezamzadeh-Ejhieh, A., **2018**. A pn junction NiO–CdS nanoparticles with enhanced photocatalytic activity: A response surface methodology study. *Journal of Molecular Liquids, 257*, pp.173–183.
5. Wang, S. and Peng, Y., **2010**. Natural zeolites as effective adsorbents in water and wastewater treatment. *Chemical Engineering Journal*, *156*(1), pp.11–24.
6. Li, X.Z., Liu, H., Cheng, L.F. and Tong, H.J., **2003**. Photocatalytic oxidation using a new catalyst TiO_2 microsphere for water and wastewater treatment. *Environmental Science & Technology*, *37*(17), pp.3989–3994.
7. Metes, A., Kovačević, D., Vujević, D. and Papić, S., **2004**. The role of zeolites in wastewater treatment of printing inks. *Water Research*, *38*(14–15), pp.3373–3381.
8. Esmaili-Hafshejani, J. and Nezamzadeh-Ejhieh, A., **2016**. Increased photocatalytic activity of Zn(II)/Cu(II) oxides and sulfides by coupling and supporting them onto clinoptilolite nanoparticles in the degradation of benzophenone aqueous solution. *Journal of Hazardous Materials*, *316*, pp.194–203.
9. Malekian, R., Abedi-Koupai, J., Eslamian, S.S., Mousavi, S.F., Abbaspour, K.C. and Afyuni, M., **2011**. Ion-exchange process for ammonium removal and release using natural Iranian zeolite. *Applied Clay Science*, *51*(3), pp.323–329.
10. Somerset, V., Petrik, L. and Iwuoha, E., **2008**. Alkaline hydrothermal conversion of fly ash precipitates into zeolites 3: The removal of mercury and lead ions from wastewater. *Journal of Environmental Management*, *87*(1), pp.125–131.
11. Metropoulos, K., Maliou, E., Loizidou, M. and Spyrellis, N., **1993**. Comparative studies between synthetic and natural zeolites for ammonium uptake. *Journal of Environmental Science & Health Part A*, *28*(7), pp.1507–1518.
12. Ahmadi, B. and Shekarchi, M., **2010**. Use of natural zeolite as a supplementary cementitious material. *Cement and Concrete Composites*, *32*(2), pp.134–141.
13. Liu, Z., Liu, Z., Cui, T., Li, J., Zhang, J., Chen, T., Wang, X. and Liang, X., **2012**. Photocatalysis of TiO_2 nanoparticles supported on natural zeolite. *Materials Technology*, *27*(3), pp.267–271.
14. Najimi, M., Sobhani, J., Ahmadi, B. and Shekarchi, M., **2012**. An experimental study on durability properties of concrete containing zeolite as a highly reactive natural pozzolan. *Construction and Building Materials*, *35*, pp.1023–1033.
15. Nezamzadeh-Ejhieh, A. and Hushmandrad, S., **2010**. Solar photodecolorization of methylene blue by CuO/X zeolite as a heterogeneous catalyst. *Applied Catalysis A: General*, *388*(1–2), pp.149–159.
16. Huang, M., Xu, C., Wu, Z., Huang, Y., Lin, J. and Wu, J., **2008**. Photocatalytic discolorization of methyl orange solution by Pt modified TiO_2 loaded on natural zeolite. *Dyes and Pigments*, *77*(2), pp.327–334.
17. Liu, Z., Liu, Z., Cui, T., Li, J., Zhang, J., Chen, T., Wang, X. and Liang, X., **2014**. Photocatalysis of two-dimensional honeycomb-like ZnO nanowalls on zeolite. *Chemical Engineering Journal*, *235*, pp.257–263.
18. Batistela, V.R., Fogaça, L.Z., Fávaro, S.L., Caetano, W., Fernandes-Machado, N.R.C. and Hioka, N., **2017**. ZnO supported on zeolites: Photocatalyst design, microporosity and properties. *Colloids and Surfaces A: Physicochemical and Engineering Aspects*, *513*, pp.20–27.
19. Babaahamdi-Milani, M. and Nezamzadeh-Ejhieh, A., **2016**. A comprehensive study on photocatalytic activity of supported Ni/Pb sulfide and oxide systems onto natural zeolite nanoparticles. *Journal of hazardous Materials*, *318*, pp.291–301.
20. Koohestani, H. and Sadrnezhaad, S.K., **2016**. Improvement in TiO_2 photocatalytic performance by ZrO_2 nanocompositing and immobilizing. *Desalination and Water Treatment*, *57*(58), pp.28450–28459.
21. Mohammadyari, P. and Nezamzadeh-Ejhieh, A., **2015**. Supporting of mixed ZnS–NiS semiconductors onto clinoptilolite nano-particles to improve its activity in photodegradation of 2-nitrotoluene. *RSC Advances*, *5*(92), pp.75300–75310.
22. Brazlauskas, M. and Kitrys, S., **2008**. Synthesis and properties of CuO/Zeolite sandwich type adsorbent-catalysts. *Chinese Journal of Catalysis*, *29*(1), pp.25–30.
23. Koohestani, H., **2019**. Photocatalytic performance of rod-shaped copper oxides prepared by spin coating. *Micro and Nano Letters*, *14*, pp.339–343.
24. Bhuvaneshwari, S. and Gopalakrishnan, N., **2016**. Hydrothermally synthesized copper oxide (CuO) superstructures for

ammonia sensing. *Journal of Colloid and Interface Science*, *480*, pp.76–84.

25. Nezamzadeh-Ejhieh, A. and Salimi, Z., **2010**. Heterogeneous photodegradation catalysis of o-phenylenediamine using CuO/X zeolite. *Applied Catalysis A: General*, *390*(1–2), pp.110–118.

26. Mekatel, E.H., Aid, A., Nibou, D. and Trari, M., **2015**. Adsorption of methyl orange on nanoparticles of a synthetic zeolite NaA/CuO. *Comptes Rendus Chimie*, *18*(3), pp.336–344.

27. Koohestani, H. and Sadrnezhaad, S.K., **2016**. Photocatalytic degradation of methyl orange and cyanide by using TiO_2/CuO composite. *Desalination and Water Treatment*, *57*(46), pp.22029–22038.

28. Koohestani, H., **2019**. Characterization of TiO_2/WO_3 composite produced with recycled WO_3 nanoparticles from W-Ni-Fe alloy. *Materials Chemistry and Physics*, *229*, pp.251–256.

29. Onsuratoom, S., Puangpetch, T. and Chavadej, S., **2011**. Comparative investigation of hydrogen production over Ag−, Ni−, and Cu-loaded mesoporous-assembled TiO_2–ZrO_2 mixed oxide nanocrystal photocatalysts. *Chemical Engineering Journal*, *173*(2), pp.667–675.

30. Onsuratoom, S., Chavadej, S. and Sreethawong, T., **2011**. Hydrogen production from water splitting under UV light irradiation over Ag-loaded mesoporous-assembled TiO_2–ZrO_2 mixed oxide nanocrystal photocatalysts. *International Journal of Hydrogen Energy*, *36*(9), pp.5246–5261.

31. Koohestani, H., **2019**. Photocatalytic removal of cyanide and Cr(IV) from wastewater in the presence of each other by using TiO_2/UV. *Micro and Nano Letters*, *14*, pp.45–50.

32. Nezamzadeh-Ejhieh, A. and Karimi-Shamsabadi, M., **2013**. Decolorization of a binary Azo dyes mixture using CuO incorporated nanozeolite-X as a heterogeneous catalyst and solar irradiation. *Chemical Engineering Journal*, *228*, pp.631–641.

33. Nezamzadeh-Ejhieh, A. and Salimi, Z., **2011**. Solar photocatalytic degradation of o-phenylenediamine by heterogeneous CuO/X zeolite catalyst. *Desalination*, *280*(1–3), pp.281–287.

34. Ruíz-Baltazar, A., Esparza, R., Gonzalez, M., Rosas, G. and Pérez, R., **2015**. Preparation and characterization of natural zeolite modified with iron nanoparticles. *Journal of Nanomaterials*, *16*(1), p.274.

35. Nezamzadeh-Ejhieh, A. and Shirzadi, A., **2014**. Enhancement of the photocatalytic activity of ferrous oxide by doping onto the nano-clinoptilolite particles towards photodegradation of tetracycline. *Chemosphere*, *107*, pp.136–144.

36. Wu, L.-P., Li, X.J., Yuan, Z.H. and Chen, Y., **2009**. The fabrication of TiO_2-supported zeolite with core/shell heterostructure for ethanol dehydration to ethylene. *Catalysis Communications*, *11*(1), pp.67–70.

37. Naghash, A. and Nezamzadeh-Ejhieh, A., **2015**. Comparison of the efficiency of modified clinoptilolite with HDTMA and HDP surfactants for the removal of phosphate in aqueous solutions. *Journal of Industrial and Engineering Chemistry, 31*, pp.185–191.

38. Yemashova, N. and Kalyuzhnyi, S., **2006**. Microbial conversion of selected Azo dyes and their breakdown products. *Water Science and Technology*, *53*(11), pp.163–171.

39. Nezamzadeh-Ejhieh, A. and Karimi-Shamsabadi, M., **2014**. Comparison of photocatalytic efficiency of supported CuO onto micro and nano particles of zeolite X in photodecolorization of Methylene blue and Methyl orange aqueous mixture. *Applied Catalysis A: General*, *477*, pp.83–92.

Received: 11 June 2019. Accepted: 3 September 2019.